Neural Networks ▮ (▮▮▮▮) ▮▮▮–▮▮▮

Contents lists available at SciVerse ScienceDirect

Neural Networks

journal homepage: www.elsevier.com/locate/neunet

2012 Special Issue

A modular neural model of motor synergies

Kiran V. Byadarhaly, Mithun C. Perdoor, Ali A. Minai *

School of Electronic and Computing Systems, University of Cincinnati, Cincinnati, OH 45221, United States

ARTICLE INFO

Keywords:
Motor control
Motor synergies
Muscle synergies
Motor primitives
Modularity
Reservoir models

ABSTRACT

Animals such as reptiles, amphibians and mammals (including humans) are mechanically extremely complex. It has been estimated that the human body has between 500 and 1400 degrees of freedom! And yet, these animals can generate an infinite variety of very precise, complicated and goal-directed movements in continuously changing and uncertain environments. Understanding how this is achieved is of great interest to both biologists and engineers.

There are essentially two questions that must be addressed: (1) What type of control strategy is used to handle the large number of degrees of freedom involved? and (2) How is this strategy instantiated in the substrate of neural and musculoskeletal elements comprising the animal bodies? The first question has been studied intensively for several decades, providing strong indications that, rather than using standard feedback control based on continuous tracking of desired trajectories, animals' movements emerge from the controlled combination of pre-configured *movement primitives* or *synergies*. These synergies represent coordinated activity patterns over groups of muscles, and can be triggered as a whole with controlled amplitude and temporal offset. Complex movements can thus be constructed from the appropriate combination of a relatively small number of synergies, greatly simplifying the control problem.

Although experimental studies on animal movements have confirmed the existence of motor synergies, and their utility has been demonstrated in the control of fairly complex robots, their neural basis remains poorly understood. In this paper, we introduce a simple but plausible and general neural model for motor synergies based on the principle that these functional modules reflect the structural modularity of the underlying physical system. Using this model, we show that a small set of synergies selected through a redundancy-reduction principle can generate a rich motor repertoire in a model two-jointed arm system. We investigate the synergies generated by this model systematically with respect to various parameters, and compare them to those observed in experiments.

1. Introduction

Movement is the only way humans (and other animals) interact with their environment, and all forms of communication including speech, sign language, etc., are generated in conjunction with the motor system (Wolpert, Ghahramani, & Flanagan, 2001). All cognitive and sensory processes can be seen primarily as the means to generate appropriate actions. Humans exhibit a large repertoire of complex movements that allows them to interact with continuously changing and uncertain environments, but the biological basis of this ability is still not completely understood. Even the simplest movements such as reaching for a glass of water involve an enormous amount of coordination and information processing across various levels in the nervous system. The desired output in this case is the acceleration of the arm, but the motor command that produces this acceleration depends on many internal and external variables of the body including the present state of the arm, the effect of sensory feedback, parameters associated with the arm (e.g. muscle masses, moments of inertia, etc.), and the global environmental conditions under which the arm is operating. The motor system must be able to provide commands based on all these variables and in different contexts (Wolpert & Kawato, 1998). This makes motor control a complex and fascinating problem for biologists, engineers and computer scientists (Bernstein, 1967; Graziano, 2009; Pfeifer & Bongard, 2006; Schmidt & Lee, 2005).

Humans have a complex body structure with more degrees of freedom than those required to perform any particular motor task. This redundancy allows for flexible and adaptable motor behavior if all the degrees of freedom can be coordinated for task performance (Bernstein, 1967). Understanding the cognitive and biomechanical basis of this coordination has been a fascinating challenge. The complexity of this problem arises from the apparent conflict between two fundamental properties of the motor system: the ability to accomplish complex, goal-directed actions repeatedly

* Corresponding author. Tel.: +1 513 556 4783.
E-mail addresses: Ali.Minai@uc.edu, minaiaa@gmail.com (A.A. Minai).

0893-6080/$ – see front matter © 2012 Elsevier Ltd. All rights reserved.
doi:10.1016/j.neunet.2012.02.003

and accurately, and doing so with a variety of different specific movements. How do humans solve this degrees of freedom problem? And how is this to be replicated in an artificial system? These are the motivating questions for this paper.

The biological motor system is essentially a solution to a very difficult control problem. It has actuators, sensors and many layers of control, but unlike artificial control systems, it performs at a high degree of accuracy with flexibility and adaptation in spite of nonlinearities, uncertainties and many degrees of freedom (Doya, Kimura, & Miyamura, 2001). Many of the models developed for motor control reduce the redundancy by replacing the behavioral goal of a movement task with a desired trajectory that the system needs to follow in order to complete the task. In these models, there is a clear separation between the stages of *movement planning* and *movement execution*, but the variability and goal-directed corrections seen in biological motor control indicate that the system is able to distinguish, and selectively enforce, constraints required for online execution of the movement goal and pursue behavioral goals directly (Todorov & Jordan, 2002). Efforts to find methods with these attributes have led to the idea of *synergistic control* techniques, where complex movements are organized by coordination of pre-specified motor primitives – called *motor synergies* – rather than by explicit control of each degree of freedom (Bizzi, Cheung, d'Avella, Salitel, & Tresch, 2007; d'Avella & Bizzi, 2005; d'Avella, Saltiel, & Bizzi, 2003; Morasso, 1992; Muceli, Boye, d'Avella, & Farina, 2010; Mussa-Ivaldi, 1999; Ting & Macpherson, 2005; Torres-Oviedo, Macpherson, & Ting, 2006; Torres-Oviedo & Ting, 2007; Tresch, Cheung, & d'Avella, 2006; Tresch, Salitel, & Bizzi, 1999). While this does not eliminate the degree of freedom problem, it can potentially mitigate it by drastically reducing the number of controlled variables without greatly limiting useful flexibility. In this paper, we explore the synergy-based approach systematically, and develop a neural model of motor synergies for a 2-degree of freedom arm with 6 muscles, capable of performing reaching movements in a large number of directions from all of its initial postures.

This paper builds on the work reported in our paper at the 2011 International Joint Conference on Neural Networks (Byadarhaly, Perdoor, & Minai, 2011), but goes beyond that in describing a much more general and detailed model of motor synergies and a significantly enhanced algorithm for obtaining a basis set of synergies.

The rest of the paper is organized as follows: The next section describes the motivation behind the synergy model and some background information about the development of the concept. The following section describes the system model in detail and the largely phenomenological methods used to configure useful synergies (described in detail in Appendix B). The capabilities of the synergy-based motor control system are demonstrated in the Results section, which shows how simple and complex reaching movements can be constructed by combining the synergies over time.

2. Background and motivation

Researchers in the area of motor control have proposed three main types of control models: Cerebellar and adaptive control models (Albus, 1971; Marr, 1969; Schweighofer, Arbib, & Kawato, 1998a; Schweighofer, Spoelstra, Arbib, & Kawato, 1998b), basal ganglia and reinforcement learning models (Barto, 1995; Graybiel, 1995; Houk, 2005; Houk, Adams, & Barto, 1995; Houk & Wise, 1995; Sutton & Barto, 1998), and modular control models (Doya et al., 2001). Among the earliest models involving the cerebellum were the classical models of Albus (1971) and Marr (1969) who proposed that the cerebellum is a pattern recognition system that recognizes contexts for specific movements. Based on this, Ito (1993) hypothesized that the cerebellum provides a model of the body and the physical environment allowing for accurate movement control despite errors in sensory feedback. Kawato extended Ito's framework and proposed the feedback error learning architecture as a model of adaptive control by the cerebellum, consisting of a fixed linear feedback controller and an adaptive nonlinear feed-forward controller. The feedback loop corresponds to the cerebral and spinal feedback pathways while the nonlinear feed-forward controller assumes the role of an inverse model of the plant, calculating the control command necessary to achieve the desired movement trajectory (Kawato, Furukawa, & Suzuki, 1987).

The actor-critic architecture for the reinforcement learning of control tasks was proposed in the early 80's by Barto and colleagues (Sutton & Barto, 1998). This consists of an *actor* that produces stochastic action outputs and a *critic* that evaluates how good or bad the resulting states are. The neurotransmitter dopamine is known to be involved in the reinforcement of human and animal behaviors (Schultz, 2000; Schultz, Dayan, & Montague, 1997). The basal ganglia receive very strong dopaminergic inputs and, based on their anatomical organization and the data from the dopaminergic neurons, several researchers have proposed actor-critic models of the basal ganglia (Barto, 1995; Houk & Wise, 1995). These models explain the role of the basal ganglia in learning and execution of voluntary movements. Similar reinforcement learning models have successfully replicated experimental data on reward based learning (Hikosaka et al., 1999; Schultz et al., 1997).

Motor adaptation experiments such as eye-movement control indicate that multiple controllers are learned for different situations (Wolpert & Ghahramani, 1997). Experiments by Imamizu, Kuroda, Yoshioka, and Kawato (2004) and Shima and Tanji (2000) suggest that the network linking the cerebellum and the premotor cortex may be involved in selecting appropriate control modules for different conditions. Wolpert and Kawato proposed a modular control architecture called the *multiple paired forward and inverse models* (MPFIM) (Wolpert & Kawato, 1998). This architecture uses multiple pairs of forward and inverse models of the controlled object. This was extended to a reinforcement learning paradigm called *multiple-model based reinforcement learning* (MMRL) by Doya, Samejima, Katagiri, and Kawato (2000b). All these models have a multiple predictor controller(MPC) architecture (Doya, Katagiri, Wolpert, & Kawato, 2000a). When a locally linear model of the dynamics and a locally quadratic model of the reward or cost are available, a special case Of the MPC architecture called the multiple linear-quadratic controller (MLQC) architecture is obtained (Doya et al., 2000b).

Optimal control has also been used for motor coordination and control. Todorov and Jordan proposed a model in which the desired trajectory is not enforced, but feedback is used intelligently by correcting only those errors that interfere with task goals (Todorov & Jordan, 2002). Other models based on optimal control have used an iterative linear quadratic Gaussian formalism as a model for control of a redundant biomechanical system represented by the motor system (Li & Todorov, 2004; Li, Todorov, & Pan, 2004).

A very different approach to motor coordination arises from the nonlinear dynamics and complex systems framework. An important insight derived from the study of complex systems is their extensive use of modularity and multi-scale self-organization. Complex patterns can arise through the interaction of relatively simple but nonlinear modules at multiple spatial and temporal scales. The modules themselves can be configured at multiple adaptive time-scales ranging from evolution to development and learning, and organized into pre-coordinated functional motor primitives, or synergies, by the same processes (Bizzi et al., 2007; d'Avella et al., 2003; Kelso, 1995, 2009; Morasso, 1992; Mussa-Ivaldi, 1999; Tresch et al., 1999; Tresch, Salitel, d'Avella,

Please cite this article in press as: Byadarhaly, K. V., et al. A modular neural model of motor synergies. Neural Networks (2012), doi:10.1016/j.neunet.2012.02.003

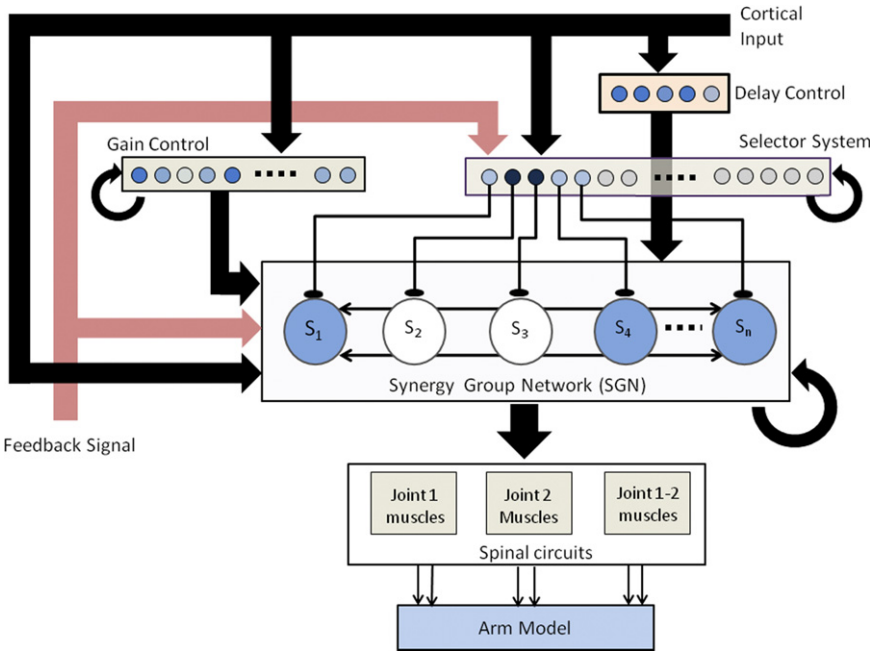

Fig. 1. Architecture of the synergy model. Differences in neuron/module shading indicate levels of activity.

& Bizzi, 2002). Complex movements can then be generated simply by triggering the appropriate synergies in coordinated fashion (Bizzi et al., 2007; d'Avella & Bizzi, 2005; d'Avella et al., 2003; Kelso, 2009; Muceli et al., 2010; Ting & Macpherson, 2005; Torres-Oviedo et al., 2006; Torres-Oviedo & Ting, 2007; Tresch et al., 2006). In this framework, motor control is seen as a purely dynamical and emergent phenomenon rather than an explicit feedback control process (Haken, Kelso, & Bunz, 1985; Kelso, 1995, 2009; Turvey, 1990; Turvey & Fonseca, 2009) (though it is modulated by feedback at many levels.) This is the motivating viewpoint of the present paper.

Though motor synergies have occasionally been invoked in computational models of motor control, they have been instantiated at a purely phenomenological level (Bullock & Grossberg, 1988; Grossberg & Paine, 2000). More recently, Schaal and colleagues have developed a concrete mathematical framework for motor primitives, and applied it very successfully to the control of high degree-of-freedom robots engaged in complex tasks (Ijspeert, Nakanishi, & Schaal, 2003; Meier, Theodorou, Stulp, & Schaal, 2011; Schaal, 2003a, 2003b; Schaal, Peters, Nakanishi, & Ijspeert, 2004). However, these primitives are purely phenomenological and are not defined in terms of neural correlates. They are also defined in terms of kinematics (Schaal, 2003b) rather than muscle forces or torques, which are the variables directly controlled by motor commands.

One of the benefits of a synergistic approach is that a large number of complex responses can be configured by the combination of a small set of synergies. These complex actions are triggered *as a whole* by a simple command input rather than detailed control signal. Not only do the synergies provide a very stable internal memory for the system and are not disturbed by variations in the system, the stability of the synergies also makes the response more robust to noise and other perturbations. It has been postulated that the synergistic, dynamical model studied in the motor system can be applied to the brain as a whole leading to the development of a complex dynamical view of all mental functions (Kelso, 2009; Minai, Perdoor, Byadarhaly, Vasa, & Iyer, 2010; Yuste, Maclean, Smith, & Lanser, 2005). This framework allows for the explanation of complex behaviors in animals from an evolutionary and developmental perspective.

We speculate that all mental functions in animals arise through the interaction of functional modules, i.e., synergies, configured at multiple levels through evolution, development and learning. The synergies in peripheral systems – the spinal cord, the brainstem, sensory receptors and the musculoskeletal system – are relatively inflexible and hard-coded (e.g., central pattern generators for locomotion, breathing, sneezing, etc.), whereas those in the core systems – neocortex, thalamus, hippocampus, cerebellum and basal ganglia – are much more flexible and reconfigurable (e.g., motor programs for complex voluntary movements). In this framework, the *peripheral synergies* of the motor system represent a *combinatorial repertoire* for the configuration of muscle force fields, whereas the *core synergies* provide the excess degrees of freedom that allow maximal *exploitation* of this repertoire. The process of animal evolution can be seen as the gradual co-complexification of the core and peripheral synergies to maintain this optimal level of exploitation, and development can be regarded as the gradual instantiation of this system. In this paper, we present a neural model for peripheral motor synergies, i.e., the repertoire, showing that it can be used as the basis for constructing complex movement using relatively simple control signals. Future work will focus on developing neural models of higher level systems that generate these control signals.

3. System description

The neural model for synergistic motor control is as shown in Fig. 1. The main parts of the model are

- The 2-joint, 6-muscle arm model.
- The spinal pattern generator circuits.
- The Synergy Group Network (SGN).
- The selection and control array comprising three networks: (a) The selector network; (b) The gain control network; and (c) The delay modulation network.

A 2-joint, 6-muscle, 2 degree-of-freedom arm is used as the body to be controlled. The joints are termed the *shoulder* joint and the *elbow* joint. The six muscles are organized into 3 agonist–antagonist pairs. One pair each connects to the shoulder and elbow joints, and the third connects with both. The arm rests on a 2-dimensional surface and is capable of moving along this

Please cite this article in press as: Byadarhaly, K. V., et al. A modular neural model of motor synergies. Neural Networks (2012), doi:10.1016/j.neunet.2012.02.003

surface. This model has been used widely in previous research on motor control, e.g., Karniel and Inbar (1997).

The muscles receive input from the alpha motor neurons in the spinal circuit which causes them to either lengthen or shorten, resulting in movement of the arm and change in the shoulder and joint angles, θ_1 and θ_2, respectively. Thus, the *posture* of the arm can be represented in (θ_1, θ_2) coordinates. A muscle is modeled mechanically as a spring–mass–damper system using a Hill-type framework derived from the previous work of Karniel and Inbar (1997) and Massone and Myers (1996).

Each muscle in the model arm is controlled by signals from the alpha motor unit of a spinal circuit. The spinal circuits are, in turn, driven by signals from the SGN, mediated by interneurons and stretch receptor feedback in the spinal circuits. The SGN is a modular network comprising *synergy groups*, each of which is itself a recurrent network of several interacting *modules*. Activation patterns are embedded as attractors within each module, and the interaction of the modules within the group results in a signature spatiotemporal response pattern for each synergy group. This represents the synergy or motor primitive encoded by that group.

Each of the synergy groups is held inactive by default through an inhibitory connection, and can be triggered to participate in a motor action by a signal from the *selector network* (SN). The selector network is a recurrent attractor network that sends enabling signals to each synergy group, thus controlling the *combination* of synergies deployed at a given time. Through learning, the selector network is expected to embed useful synergy combinations as attractors, with appropriate patterns being triggered sequentially by higher-level motor commands. Each synergy, i, triggered by the selector network is modulated further by the *gain control network* (GCN), which scales the response amplitude, k_i, of the selected synergy, and the *delay control network* (DCN), which controls the delay, δ_i, with which a selected synergy is deployed. The SGN has a fixed pattern of projection onto the spinal circuits of the six muscles; this is termed the *muscle map* of the system.

The output from the SGN is a spatiotemporal pattern of brief square-wave signals that is provided to the spinal networks through the muscle map, and drives the appropriate spinal networks, thus leading to muscle activation and movement. The property of the movement which is of most interest to us is the trajectory of the end point of the arm. This would correspond to a drawing or reaching action by an attached end effector. The spinal circuits, the SGN and the control networks are described below in greater detail. The arm model is described in Appendix A.

The model described here does not include any visual or somatosensory feedback except that from muscle stretch sensors; nor does it include efference copy-based modulation, which is known to exist in the motor system. Thus, the current model should not be expected to produce goal-directed trajectories with the precision or control seen in actual animals. The goal in this paper is to show how peripheral motor synergies can be instantiated in a modular neural substrate, and how a small number of such synergies can, in principle, provide a comprehensive and efficient repertoire of movements.

3.1. Spinal circuits

Spinal circuits form the output stage of the motor neural system. While spinal circuits are known to include many types of neurons, we use the simplified model shown in Fig. 2. It has been derived from the limb controller model of Orlovsky, Deliagina, and Grillner (1999), which consists of a rhythm generator and an output stage which does not take part in the generation of the rhythm (Feldman & Orlovsky, 1975; Pratt & Jordan, 1980). The output stage activates a pair of agonist–antagonist muscles and can be seen as a functional unit activated by both the brain and

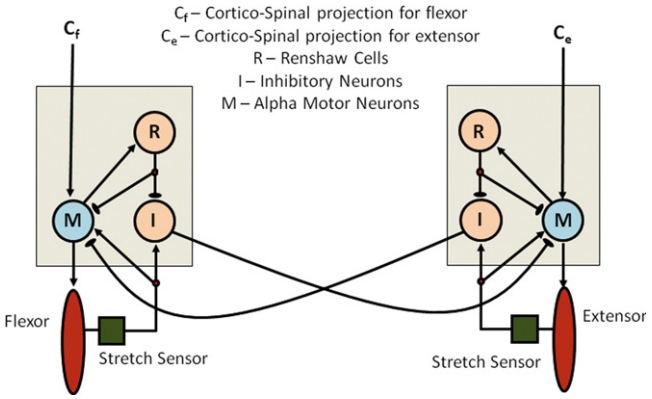

Fig. 2. The spinal circuit.

the spinal cord. In Orlovsky's model, the output stage comprises a pair of alpha motor neurons that activate the muscles, a pair of inhibitory neurons receiving afferent stretch signals from the muscle pair, a pair of Renshaw cells and a pair of gamma motor neurons. The inhibitory neuron provides inhibitory feedback to the agonist alpha motor neuron when the antagonist muscle is stretched. The gamma motor neurons affect the sensitivity of the stretch-receptive muscle spindle afferents. The Renshaw cells are also inhibitory and receive excitatory signals from the alpha motor neurons. Our system is similar to Orlovsky's except that gamma motor neurons are excluded and the sensitivity of the stretch receptive muscle spindles is fixed. It should be noted that, while we use the term "neuron" in our description, the units in our model are better seen as neural assemblies (e.g., motor pools).

All three types of neurons in spinal circuits (alpha motor neurons, inhibitory neurons and Renshaw cells) have a sigmoidal activation function, and are implemented using continuous time dynamics. The activity of a neuron i is given by an equation of the form:

$$\tau_i dV_i/dt = -V_i + \sum_k W_{jk} Y_k + I_i^q \tag{1}$$

where τ_i is the time constant for neuron i, W_{jk} is the synaptic weight from afferent neuron k to neuron i, Y_k is the output of neuron k, and I_i^q is the extra-spinal input to neuron i, where $q = \alpha$ if i is an alpha motor neuron and $q = \text{inh}$ if it is an inhibitory neuron; Renshaw cells do not get extra-spinal input. The output of i is given by:

$$Y_i = \frac{1}{1 + e^{-V_i}} \tag{2}$$

which can be seen as the firing rate of the neuron. If $Y_i < 0.01$ then $Y_i = 0$.

The extra-spinal input to alpha motor neurons comes from the SGN units through the weights encoded in the muscle map and is given by

$$I_i^\alpha = \sum_j W_{ij} Y_j - B^s \tag{3}$$

where Y_j is the output of SGN neuron j which affects the muscle through weight W_{ij} and B^s is the bias for the spinal circuits, which is set to the value 5 in the simulations.

The extra-spinal input to the inhibitory neuron is the muscle stretch which is calculated as:

$$I_j^{\text{inh}} = \frac{L - L_{\text{rest}}}{L_{\max} - L_{\text{rest}}} \tag{4}$$

where L is the current length of the muscle, L_{rest} is the length of the muscle when there is no stretch, and $L_{\max}$ is the maximum possible

Please cite this article in press as: Byadarhaly, K. V., et al. A modular neural model of motor synergies. Neural Networks (2012), doi:10.1016/j.neunet.2012.02.003

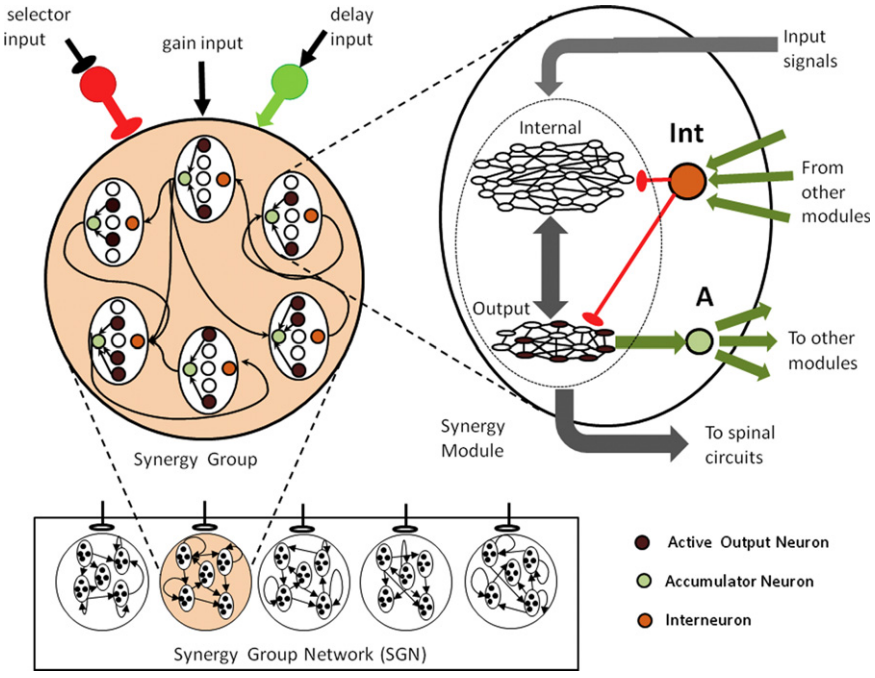

Fig. 3. Architecture of the Synergy Group Network.

length of the muscle:

$$L_{\text{rest}} = \frac{L_{\max}}{2}. \tag{5}$$

Based on these, we get $-1 \leq I_i^{\text{inh}} \leq 1$.

3.2. The Synergy Group Network

Fig. 3 shows the Synergy Group Network. It is organized into synergy groups comprising interacting modules, each of which is itself a recurrent neural network. The intra-module connectivity is dense while inter-module connections are sparse and are mediated through interneurons (see below). Each module embeds a unique neural activity pattern as an attractor. By varying inter-module connectivity, the synergy group thus has the capability of constructing many different group-wide attractors using the module attractors as building blocks. It is, in fact, a *combinatorial reservoir* of modular attractors. The attractor actually constructed by the inter-modular weights represents the group's embedded synergy pattern.

As shown on the upper right of Fig. 3, the primary neurons in a module are divided into two groups: *internal neurons*, which only have recurrent connections within the group, and *output neurons*, which send output to the spinal circuits. All these neurons receive *motor command inputs* from higher level systems (e.g., the motor cortex), which are not included in the current model. The internal neurons interact recurrently with all neurons in the group. In addition to these primary neurons, each module has two interneurons: (1) an excitatory *accumulator neuron* that receives input from the module's output neurons, and (2) an inhibitory interneuron that receives input from the accumulator neurons of the other modules and modulates the charging rate of neurons in the module. This setup provides natural delays in the relative firing times of the neurons in individual modules within the same group. The modules that fire early inhibit the firing of other modules resulting in different timing of the signals to the muscles.

The attractors are embedded in the modules through recurrent weights specified via a covariance-based rule. For a particular module m in a group g, the recurrent weights are set by the following relation

$$W_{jk}^m = \frac{1}{N}\sum_{q=1}^{N}(Y_{jq}^m - \bar{Y_j^m})(Y_{kq}^m - \bar{Y_k^m}) \tag{6}$$

where W_{jk}^m is the synaptic weight from neuron k to neuron j in the synergy module m, Y_{jq}^m is the output of the neuron j for the attractor pattern q in synergy module m, $\bar{Y_j^m}$ is the mean activity of neuron j over all the attractor patterns for module m, and N is the number of attractor patterns stored in the synergy group.

As discussed above, synergy groups are inhibited by default via a tonically active inhibitory unit. Only if this inhibition is lifted *and* sufficient excitation provided does a synergy group become active. These two functions are controlled, respectively, by inputs from the selector network and the delay control network. When the synergy group does become active, its level of output is determined by the input it receives from the gain control network. These mechanisms are described in greater detail below.

The activity of the neuron j in module m in an active synergy group g is given by

$$V_j^m(t) = (1 - r_m^g)V_j^m(t-1) + r_m^g(t)\left(\sum_{k=1}^{n_m} W_{jk}^m Y_k^m(t-1) + I_j\right) \tag{7}$$

where V_j^m is the activity of the neuron j in module m, Y_j^m is the output of the neuron j in module m, n_m is the number of neurons in module m, and I_j is the motor command input to the neuron j. Here r_m^g represents the rate of charging of neurons in module m of group g. It is determined by the activity of the interneurons in the module, and is given by

$$r_m^g = \sum_{k=1}^{M_g} \omega_{jk}^g a_k^g \tag{8}$$

where a_k^g is the activity of the accumulator neuron for module k in group g, M_g is the number of modules in group g, and ω_{jk}^g represents the weights connecting the accumulator neuron of module j with the interneuron of module k for group g.

Please cite this article in press as: Byadarhaly, K. V., et al. A modular neural model of motor synergies. Neural Networks (2012), doi:10.1016/j.neunet.2012.02.003

The activation of the accumulator neurons for the modules in a group is given by

$$a_m^g = \overline{w}_m^g \cdot \overline{V}_m^g \tag{9}$$

where a_m^g is the accumulator neuron activity of module m in group g, $\overline{V}_m^g$ is a vector representing the activities of all output neurons of module m in group g, and $\overline{w}_m^g$ is the vector of synaptic weights connecting the output neurons of module m to its accumulator neuron.

Each neuron also has a *resource*, ρ_j, which depletes continuously while the activity of the neuron (V_j^m) remains above a threshold, θ. If ρ_j falls below a threshold θ_ρ^-, the neuron becomes refractory, allowing time for the resource to recharge. Once it charges to a level above θ_ρ^+, the neuron can fire again.

The resource depletion equation for a particular neuron j is given by

$$\rho_j(t+1) = (1-b)\rho_j(t) \quad b = 0.02. \tag{10}$$

The resource recharging equation is given by

$$\rho_j(t+1) = \rho_j(t) + c\left(1-\rho_j(t)\right) \quad c = 0.0004. \tag{11}$$

The resource in the system is used to control the duration the neuron's activity and refractoriness. This ensures that the activity pattern generated by the triggering of a synergy group has a finite duration, as is seen in actual motor synergies. We set $\theta_\rho^+ = 0.9999$ and $\theta_\rho^- = 0.1$.

The outputs, Y_j^m, of primary neurons j are determined by a competitive process, with only the K most excited neurons allowed to fire provided their activation also exceed a minimal threshold. Competition occurs separately for the internal and output neurons, and for output neurons is controlled by the input from the gain control network.

For simplicity (and given the small number of joints currently simulated), we assume that each module within the group affects a different muscle and each group as a whole activates every muscle in principle, though in practice some muscles may get no input due to zero weights.

3.3. Control networks

As shown in Fig. 1, the system has three networks that determine the deployment of synergies. Together, they control the selection, activity amplitude and temporal offset for synergies in the SGN as follows.

The *gain control network* provides input k_g to synergy group g, which sets the fraction of output neurons allowed to fire in each module of group g if the group is triggered. This, in turn, determines the strength of the signal each module sends to the spinal circuit, resulting in varying overall activation to the muscles in response to the synergy.

The *selector network* and the *delay control network* act through two interneurons that are associated with each synergy group g: a tonically active inhibitory neuron with activity z_I^g that keeps the synergy group inactive by default; and an excitatory interneuron with activity z_E^g that provides the drive necessary to activate the modules in the synergy group. When a synergy group is to be selected for activation, a binary signal, s_g, from the selector network inhibits the inhibitory interneuron, setting $z_I^g = 0$ and thus disinhibiting group g. However, it cannot actually become active until it receives sufficient excitation $z_E^g \geq \theta_z$ from the excitatory interneuron whose excitation is controlled by a signal, δ_g, from the delay control network. Thus, the switching of group g can be described through a gating variable, γ_g with the following logic:

$$\gamma_g(t) = s_g(t)[z_E^g(t) \geq \theta_z]. \tag{12}$$

Only if $\gamma_g = 1$ can group g be triggered, with the amplitude of the output controlled by k_g. We assume for simplicity that projection neurons in all three control networks are in one-to-one correspondence with synergy groups, but this is not essential.

For each synergy deployment, the excitatory interneuron is initialized to $z_E^g(0) = \delta_g$ and then charges as follows:

$$z_E^g(t+1) = z_E^g(t) + \tau_z\left(1 - -z_E^g(t)\right) \tag{13}$$

where $\tau_z = 0.007$ is a rate parameter.

An important feature of the control networks is that they control the SGN via patterns of activity across their own neurons. Thus, given the repertoire of synergies in the SGN and a particular embodiment, a repertoire of movements can be embedded in the networks as attractor patterns, each which can then be triggered as unitary entities by cortical and sensory feedback signals. Thus, the control networks can be seen as encoding "higher-level synergies" to elicit desired movements from lower-level synergies (Giszter, Moxon, Rybak, & Chapin, 2001; Kelso, 2009; Yuste et al., 2005).

3.4. Configuration of the synergies

The evolutionary–developmental approach that motivates our model is based on the idea that inflexible peripheral synergies are at least partly "hard wired" by genetics and development—much as the central pattern generators underlying walking, breathing, sneezing, etc., are. This gets support from the work of Ting and Macpherson (2005) and Torres-Oviedo et al. (2006); Torres-Oviedo and Ting (2007), who found that, in both cats and humans, synergies across different individuals are remarkably similar. We hypothesize that this similarity reflects the very strong constraints imposed by embodiment and the anatomy of spinal circuits. With this principle in mind, we use a heuristic search process to identify a small set of *basis synergies* for our system, attempting to capture the effect of evolutionary and developmental configuration at a phenomenological level. The heuristic is based on two principles:

1. *Maximum coverage*: Together, the synergies should cover movement in all directions from all points in the field of motion.
2. *Minimum redundancy*: The synergies found should be pairwise significantly different from each other.

In addition to this, we also impose an *admissibility constraint* that, for the same amplitude gain, the trajectories generated by each basis synergy in isolation should be of a similar moderate length and have minimal curvature.

For simplicity, we assume that all the synergy groups have 6 modules—each one projecting to the spinal circuit for a unique target muscle. Thus, each synergy group projects to all 6 muscles and the muscle map has a simple one-to-one structure. Each module has n_m neural units—n_m^I internal and n_m^o output. A module embeds one of three *canonical attractors*: (1) a strong attractor, A_s; (2) A weak attractor, A_w; and (3) A zero attractor, A_0. Each attractor has the same number of active bits across all n_m neurons in the module, but the output neurons activated by each attractor are distinct. The weights from these neurons to the spinal networks are such that the attractors provide a strong, weak or zero activation to the target muscle. With 6 modules and 3 attractors per module, each synergy group can encode 729 possible attractor combinations. These are not identical for each synergy group, though, because the inter-module weights within each synergy group are fixed at different random values.

To find a good set of synergies, 49 regularly spaced points are identified in posture space, and the region around each posture is divided radially into eight equal zones, $Z_1; \ldots; Z_8$ of 45° each. If triggering synergy i at posture k causes movement into zone Z_j, the synergy is said to *reach* Z_j at k. A set of synergies is said to *span* posture k if they reach at least 3 zones at the posture

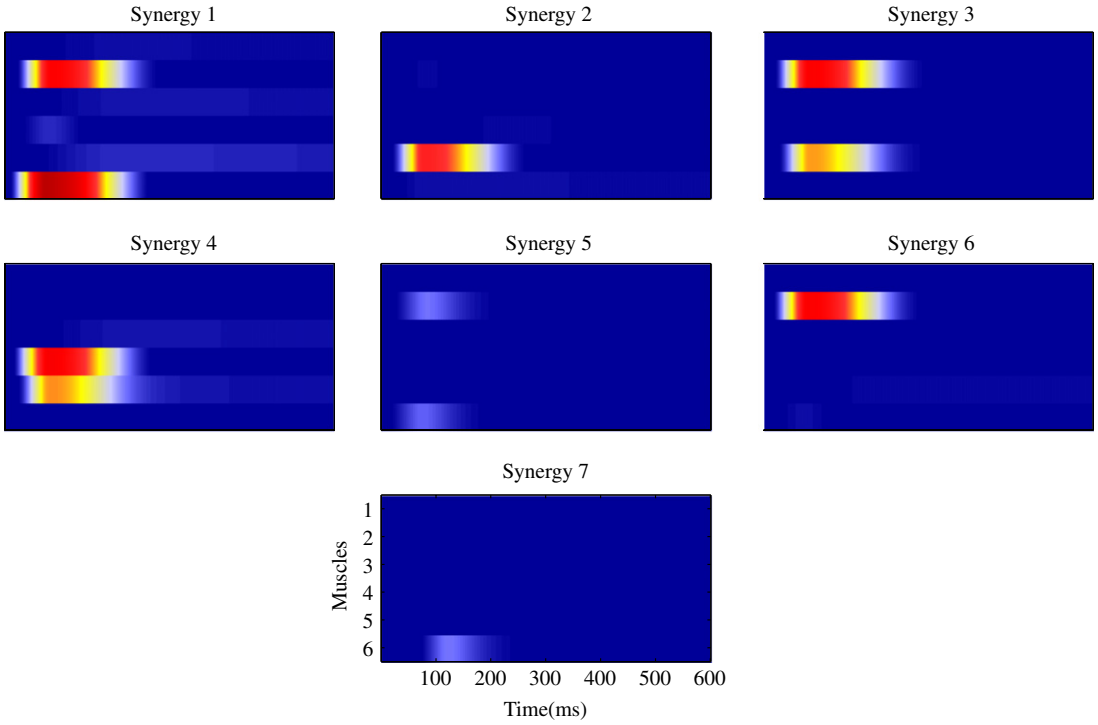

Fig. 4. The variation of the 7 muscle synergies across all six muscles. The *y* axis represents the muscles and the *x*-axis shows time. The different intensities depict the strength of the muscle force generated by the synergy.

with one intervening zone between each of the three. Some extremal postures can be spanned by covering fewer zones. A set of synergies that together span all 49 postures is said to *cover* the postures and is termed *complete*. The goal of synergy configuration is to find a minimal complete set of synergies. The resulting synergies comprise a *synergy basis set*, and movements in all directions can, in principle, be produced from any posture by the combination of subsets of these synergies with amplitude and delay modulation. Using a heuristic elimination process described in detail in Appendix B, we obtained a final canonical basis set of 7 synergies.

4. Results

The canonical set of 7 synergies was implemented in a 7-group SGN and used for all subsequent simulations as described below. The following issues were addressed through these simulations.

1. Can synergies similar to those seen in the experimental studies (Bizzi et al., 2007; d'Avella et al., 2003; Tresch et al., 1999, 2002) be generated by the model? If so what sort of arm movements do they produce at different initial postures?
2. What is the effect of the gain and delay parameters on the muscle force generated in the arm and the trajectory of the arm?
3. Can synergies be combined and modulated to generate predictable trajectories?
4. Is this system capable of producing complex sequential movements?

Fig. 4 shows the strength of activation of muscle forces produced by all of the configured synergies. It is evident from the figure that each synergy targets a few muscles strongly but also activates some of the other muscles to varying degrees. Synergies 1, 3, and 4 affect 2 muscles strongly and a few others weakly, while synergies 2 and 6 affect one of the muscles strongly and other muscles weakly. Synergies 5 and 7 provide relatively weak activation to one of the muscles while not affecting any other muscle. It can also be observed that, within the synergies, different muscles are activated at different times due to the delay inherent in each synergy.

Fig. 5 plots the movement of the arm as a result of the activation of the muscle system by synergies 1, 2, 3 and 4 from 49 initial postures of the arm. Each synergy results in a certain characteristic movement from all the initial configurations of the arm. The figure shows that the movements produced by each synergy vary smoothly with change in initial, suggesting a smooth force field. It is also clear from the figure that the synergies produce movements in very different directions.

Fig. 6 shows the movements produced by all 7 synergies from the 49 initial postures. From each posture, the repertoire of 7 synergies allows movement in multiple linearly independent directions with low curvature trajectories of roughly similar lengths, thus satisfying the criteria used to obtain the set of basis synergies.

The plots in Fig. 7 show the effect of change in gain and delay values on the muscle forces produced by pure synergies. Part (a) of the figure shows that, with decrease in the gain, the magnitude of the muscle force also decreases. This force is controlled by the number of active output neurons in the modules of each synergy group, which is determined by the gain input to that group. The figure shows that with lower amplitude, the synergy has much weaker effect on the movement of the arm, and that this effect is very significant when synergies are combined. Part (b) of the figure shows the effect of delay modulation on the muscle forces. As the delay value is increased, the excitatory neuron takes more time to charge up thus resulting in the delayed activation of the muscle.

As shown in Fig. 6, the basic set of synergies configured in the system are individually capable of producing movements in various directions from a large number of initial configurations. Fig. 8 shows that combining multiple synergies with different gains leads to monotonic – albeit slightly nonlinear – interpolation of trajectories between those produced by each synergy acting alone. The plots demonstrate this using a combination of synergies 2 and 4 (plot (a)) and synergies 3 and 6 (plot (b)), both from the same

Please cite this article in press as: Byadarhaly, K. V., et al. A modular neural model of motor synergies. Neural Networks (2012), doi:10.1016/j.neunet.2012.02.003

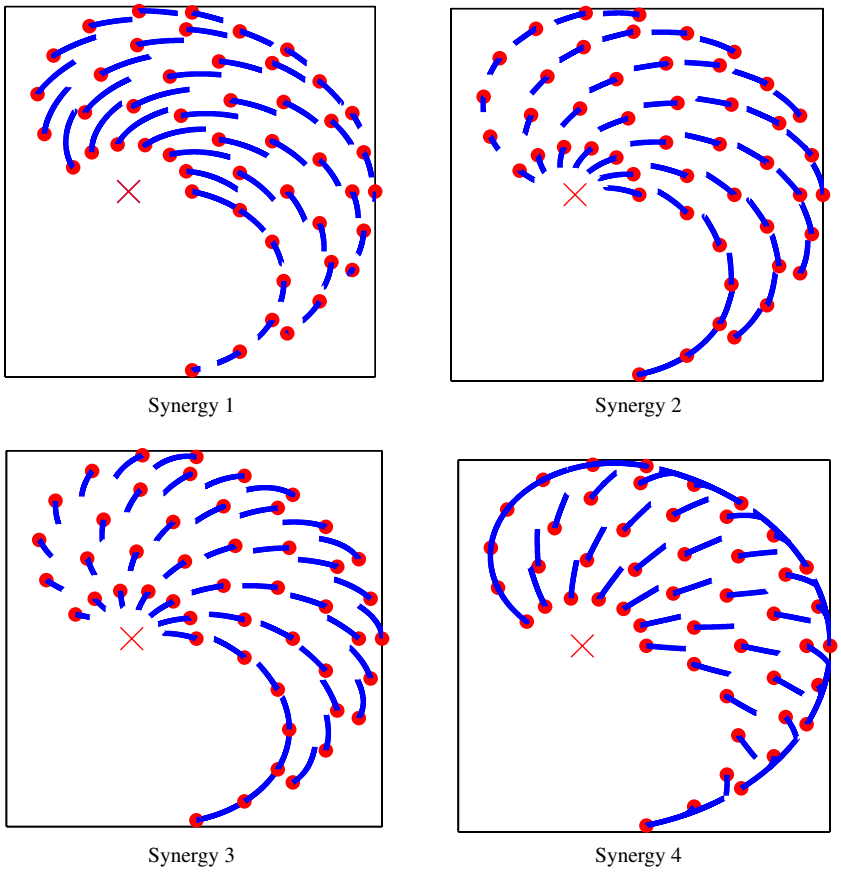

Fig. 5. Trajectories of the end point of the arm resulting from the individual activation of synergies 1, 2, 3 and 4 from all 49 initial postures. The dots indicate the initial point of the arm. The shoulder joint is at coordinates [0, 0].

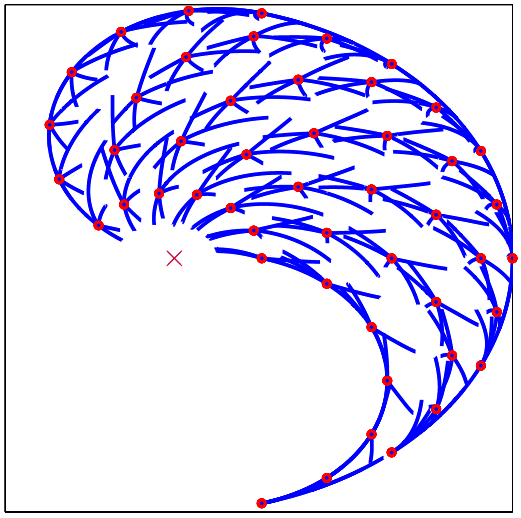

Fig. 6. Trajectories of the end point of the arm as a result of individual activation of all 7 basis synergies from all 49 initial postures. The dots in the plot refer to the initial point of the arm, and the shoulder joint is at coordinates [0, 0].

initial posture. Similar results are obtained for other combinations at this and other postures. It should be noted that a gain value of 0.5 signifies that the synergy is applied at full strength and lower gain values indicate application at lower strengths. The results shown in this figure demonstrate that, once a small but complete repertoire of synergies is found for the system, they can be combined at different gain values to produce movement in virtually any feasible direction from any posture.

Fig. 9 shows the effect of delays on the combination of synergies. Synergies 2 and 4 are combined with different values of delay between them. In Part (a) of the figure, synergy 4 is applied first and synergy 2 is applied at different values of delay after synergy 4. Similarly in part (b) of the figure synergy 2 is applied first followed by synergy 4 with different values of delay. The type of movements produced vary with delay in a systematic way though the synergies being combined are the same.

Finally, Fig. 10 shows that the model described in this paper is capable of producing complex figures by activating the system with the right sequence of synergy combinations at a chosen set of initial postures with specific sets of amplitudes and delays. Each element of the sequence is an appropriate synergy or a combination of synergies that would result in a drawing in a desired direction and, in this case, is found by explicit interpolation for each of the intermediate initial configurations involved in the figure. A system capable of learning, encoding and replaying complex response sequences will be added to the model in the future. We have recently developed preliminary models for such sequence learning neural systems (Byadarhaly, Perdoor, Vasa, Fernandez, & Minai, 2009; Vasa, Ma, Byadarhaly, Perdoor, & Minai, 2010).

5. Conclusion and future work

In this paper, we have shown how a set of peripheral motor synergies can be configured in a simple but biologically plausible neural model. The resulting system provides an *exploitable repertoire* of motor primitives that a higher level system can use to construct complex movements. The preliminary work described above indicates that this is indeed possible. We are currently

Please cite this article in press as: Byadarhaly, K. V., et al. A modular neural model of motor synergies. Neural Networks (2012), doi:10.1016/j.neunet.2012.02.003

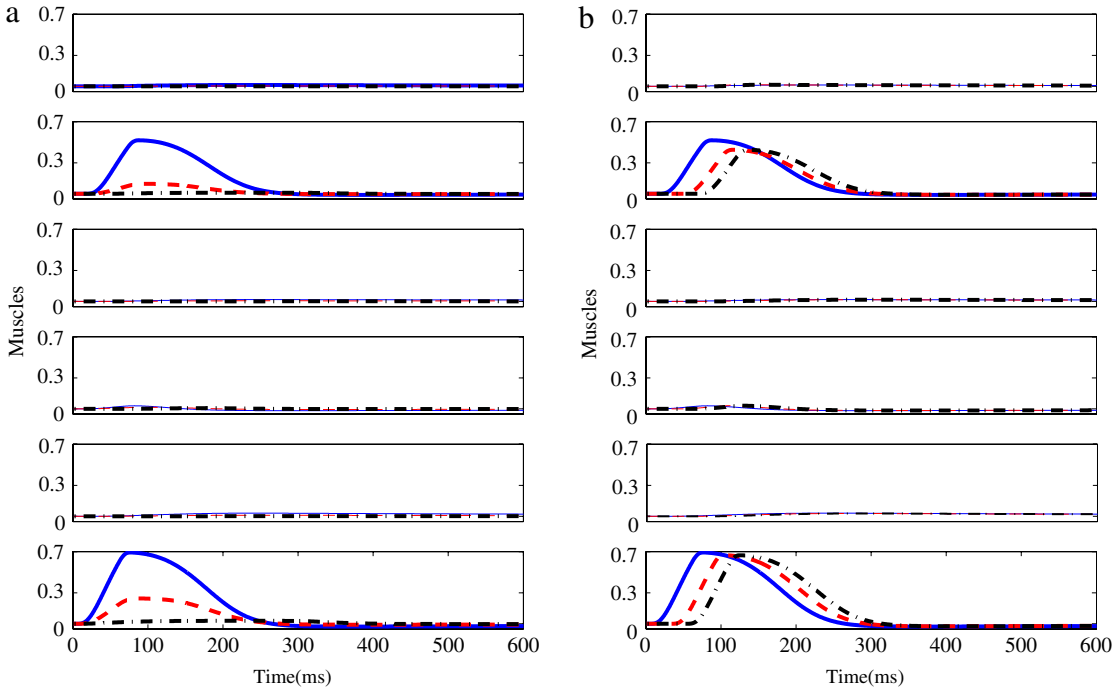

Fig. 7. (a) Forces for all 6 muscles activated by synergy 1 with gain of 0.5 (solid blue line), 0.3 (dashed red line) and 0.1 (dot–dash black line). (b) Forces for all 6 muscles activated by synergy 1 with a delay of 0 (solid blue line), 0.1 (dashed red line) and 0.2 (dot–dash black line). (For interpretation of the references to colour in this figure legend, the reader is referred to the web version of this article.)

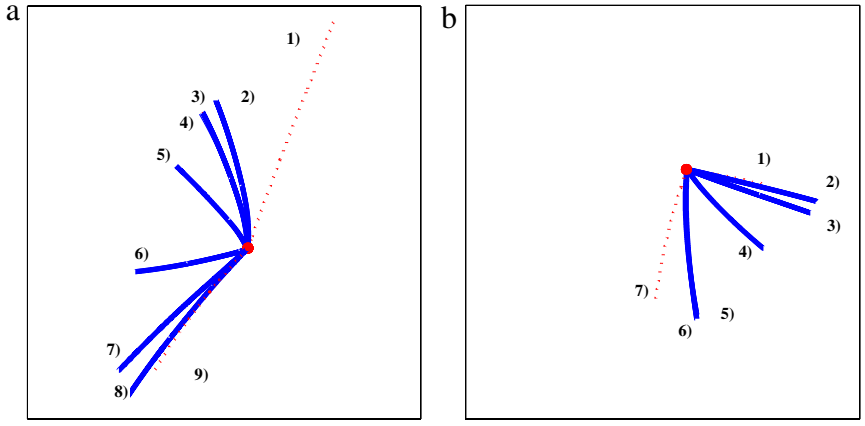

Fig. 8. Effect of combination of synergies (a) Combination of synergies 2 and 4 with different gains from a specific posture. The dotted lines show the trajectories generated by the two synergies applied alone with a gain of 0.5 and the solid lines show those obtained through the combination of the synergies. The gain values for synergies 2 and 4, respectively, are (1) (0, 0.5) (2) (0.2, 0.5) (3) (0.3, 0.5) (4) (0.5, 0.5) (5) (0.5, 0.4) (6) (0.5, 0.3) (7) (0.5, 0.2) (8) (0.5 0.1) (9) (0.5, 0). Both synergies are triggered without delay. (b) Trajectories obtain through combination of synergies 3 and 6 with respective gain values (1) (0, 0.5) (2) (0.2, 0.5) (3) (0.3, 0.5) (4) (0.4, 0.5) (5) (0.5, 0.5) (6) (0.5, 0.2) (7) (0.5 0).

working on systems that build higher-order synergies using the primitives described here as building blocks. In particular, we are focusing on developmental models that allow more complex control to emerge over time in a brain-body system of gradually increasing complexity. Results from this work will be discussed in future reports.

Appendix A. Musculoskeletal model of the 2-jointed arm

This appendix describes the musculoskeletal model for the 2-jointed arm used in this study. The model is based on the work of Karniel and Inbar (1997) and Massone and Myers (1996).

The muscle model is the widely used Hill model (Karniel & Inbar, 1997; Massone & Myers, 1996). It comprises two sets of contractile and damping elements—one in series and the other in parallel. The length of the muscle is given by $x(t)$ and the length of the contractile element by x_0, the spring constants of the series and parallel contractile elements by K_s and K_p, respectively. The viscosity factors of the damping elements are given by B (series element) and B_p (parallel element). The parallel contractile element is used to maintain a posture or muscle length at a steady state and we do not use it in our system since we are not concerned with movements that require steady maintenance of the posture.

The dimensionless force, $F_o(t)$, applied to the muscle is generated by the output, Y^m, of the muscle's alpha motor neuron via the low-pass filter $1/(1+\tau_n s)$. This is converted into force T_o measured in Newtons via a scale factor. For clarity, the dependence on t is not shown explicitly in the rest of this appendix unless necessary.

Please cite this article in press as: Byadarhaly, K. V., et al. A modular neural model of motor synergies. Neural Networks (2012), doi:10.1016/j.neunet.2012.02.003

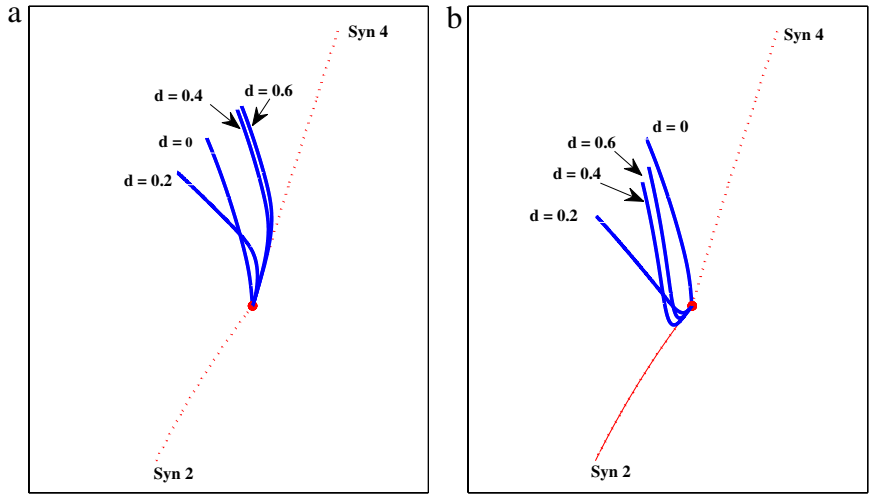

Fig. 9. Effect of changing relative delays with the combination of synergies 2 and 4 from a particular posture. (a) Synergy 2 delayed with respect to synergy 4. The dotted lines show the trajectories produced by the synergies acting alone while the solid lines show those produced by combination of the synergies at delay values denoted by *d*. (b) The same process as shown in plot (a) but with synergy 4 delayed with respect to synergy 2.

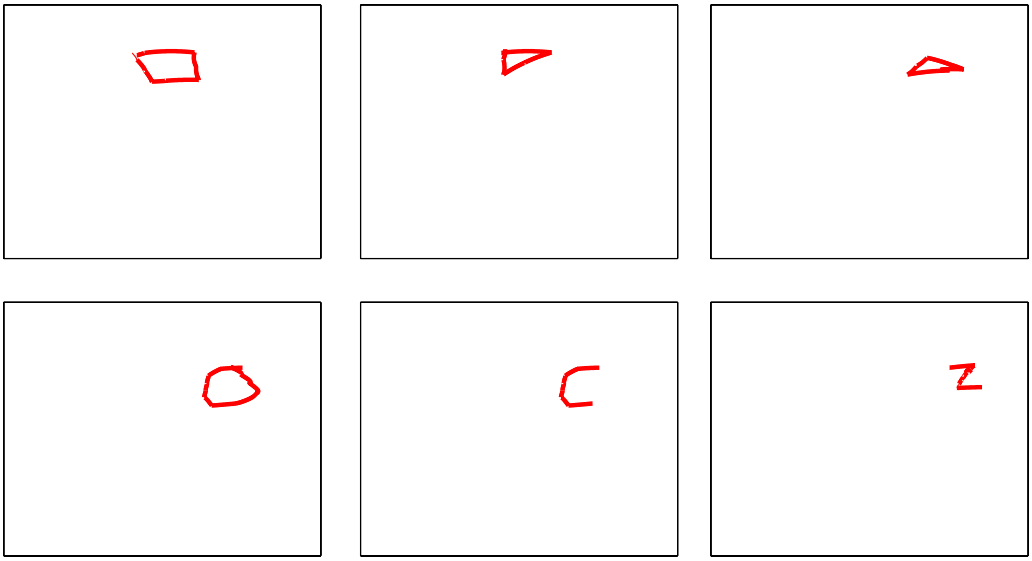

Fig. 10. An assortment of complex figures drawn by the arm when activated by various sequences of synergy combinations.

The muscle equations are

$$\frac{dF_0}{dt} = \frac{Y^m - F_0}{\tau_n} \tag{14}$$

$$T_0 = F_0 F_{\max} \tag{15}$$

where τ_n is the time constant and $F_{\max}$ is the maximum force that can be generated by the muscle

$$B\frac{dx_0}{dt} + T_0 = K_s(x - x_0) \tag{16}$$

$$F_m = B_p\frac{dx}{dt} + K_p x + K_s(x - x_0) \tag{17}$$

where F_m is the actual force generated by the muscle.

The values of $F_{\max}$ for the shoulder, elbow and double joint muscles are set to 100 N, 87.5 N and 125 N, respectively. The remaining parameter values are set as: $B_p = 0.2$ N/m/s, $K_s = 30$ N/m, $K_p = 0$, $\tau_n = 0.04$.

The viscosity factor B, is often assumed to be a constant (Jordan, Flash, & Arnon, 1994; Massone & Myers, 1996). However, we use a nonlinear version of the Hill model, which is more accurate (Flash & Hogan, 1985; Karniel & Inbar, 1997; Krylow & Zey Zymer, 1997; Schlutz, Faulkner, & Kadhireshan, 1991; Winters & Stark, 1987). Thus, B is given by

$$B = \begin{cases} (a_m T_0)/(b_m + v), & \text{if } v \geq 0 \\ a'_m T_0 & \text{if } v < 0 \end{cases} \tag{18}$$

where $a_m = 1.25$, $a'_m = 3$, $b_m = 1$, and $v = -x_0/m$. The values of the parameters are taken from the Karniel and Inbar (1997) and Massone and Myers (1996) papers.

The torques generated on the arm by the muscle force are calculated as

$$T_1 = F_{1-\text{flex}} - F_{1-\text{ext}} + 0.6F_{3-\text{flex}} - 0.6F_{3-\text{ext}} \tag{19}$$

$$T_2 = F_{2-\text{flex}} - F_{2-\text{ext}} + 0.4F_{3-\text{flex}} - 0.4F_{3-\text{ext}}. \tag{20}$$

Here F_1, F_2 and F_3 are forces generated by the shoulder, elbow and 2-joint muscles, respectively, and *flex* and *ext* indicate the flexor and extensor muscles, respectively. The torques cause the movement of the arm resulting in the change of the arm posture $[\theta_1, \theta_2]$ and the muscle length. The relationship between the

Please cite this article in press as: Byadarhaly, K. V., et al. A modular neural model of motor synergies. Neural Networks (2012), doi:10.1016/j.neunet.2012.02.003

posture and the muscle length is given by

$$X_{1-\text{flex}} = (\pi - \theta_1)\mu \tag{21}$$

$$X_{1-\text{ext}} = (\pi + \theta_1)\mu \tag{22}$$

$$X_{2-\text{flex}} = (\pi - \theta_2)\mu \tag{23}$$

$$X_{2-\text{ext}} = (\pi + \theta_2)\mu \tag{24}$$

$$X_{3-\text{flex}} = (\pi - \theta_1)\mu + (\pi - \theta_2)\mu \tag{25}$$

$$X_{3-\text{ext}} = (\pi + \theta_1)\mu + (\pi + \theta_2)\mu \tag{26}$$

where X_1, X_2 and X_3 are the lengths of the shoulder, elbow and the 2-joint muscles, respectively, and μ is the mean moment arm, set to 0.05 m (5 cm).

The dynamics of the arm relating the input torques to the postures are taken from Asada and Slotine (1986), and are given by

$$T_1 = H_{11}\frac{d^2\theta_1}{dt^2} + H_{12}\frac{d^2\theta_2}{dt^2} - h\left(\frac{d\theta_2}{dt}\right)^2 - 2h\frac{d\theta_1}{dt}\frac{d\theta_2}{dt} + G_1 \tag{27}$$

$$T_2 = H_{22}\frac{d^2\theta_2}{dt^2} + H_{12}\frac{d^2\theta_1}{dt^2} + h\left(\frac{d\theta_1}{dt}\right)^2 + G_2 \tag{28}$$

where

$$H_{11} = M_1\frac{L_1^2}{4} + M_1\frac{L_1^2}{12} + M_2\left(L_1^2 + \frac{l_2^2}{4} + L_1L_2\cos(\theta_2)\right) + M_2\frac{L_2^2}{12} \tag{29}$$

$$H_{22} = M_2\frac{L_2^2}{4} + M_2\frac{L_2^2}{12} \tag{30}$$

$$H_{12} = M_2L_1L_2\cos(\theta_2) + M_2L_2^2/2 + M_2\frac{L_2^2}{4} + M_2\frac{L_2^2}{12} \tag{31}$$

$$h = M_2L_1L_2\sin(\theta_2)/2 \tag{32}$$

where $M_1 = 2.52$ kg and $M_2 = 1.2$ kg represent the mass of the arm segments, $L_1 = L_2 = 0.3$ m are lengths of the arm segments, and G_1, G_2 represent the gravitational effects of the arm which are set to 0 since the arm rests on a surface. The arm is constrained in its movement and the joint angles are limited to the ranges $-75^\circ \le \theta_1 \le 75^\circ$ and $0^\circ \le \theta_2 \le 165^\circ$.

The property of the movement that we are interested in is the trajectory of the end point of the arm. This is equivalent to the drawing drawn by the arm if a pen was attached to its end point. The end point position of the arm is related to the present posture $[\theta_1, \theta_2]$ of the arm by the following forward kinematic relation

$$X = L_1\cos(\theta_1) + L_2\cos(\theta_1 + \theta_2) \tag{33}$$

$$Y = L_1\sin(\theta_1) + L_2\sin(\theta_1 + \theta_2). \tag{34}$$

Appendix B. Procedure for constructing the synergy basis set

As described in Section 3.4, the motor synergies are encoded within the modular synergy groups of the Synergy Group Network(SGN). Each synergy group, g, comprises six modules, each projecting uniquely to one of the six muscles. Each module embeds three attractors (A_s, A_w and A_0), giving a total of $N_T = 729$ possible attractor combinations, which we term the *initial synergy set*, S_0, since each attractor combination is a potential synergy. The internal delays for the modules, determined implicitly by the $\bar{\omega}_m^g$ weights, are set randomly to fixed values.

The selection of the final set of basis synergies, based on the principles of *maximum coverage* and *minimum redundancy*, proceeds in six stages as follows. The target count of synergies is set to N_{target}—typically less than less that 1% of the total number of possible SGN attractor combinations. The following iterative procedure is then run to obtain the basis synergy set.

Stage I: *Initial configuration of data matrices*:

In this stage, data is obtained for all N_T synergies in S_0 from all 49 postures, resulting in three data matrices:

The 3-dimensional, $N_T \times 49 \times 8$ Zone Performance Matrix, M^T_{spz}, is calculated by giving each synergy as the input to the arm in all 49 postures and noting the zone of the resulting trajectory is noted (the subscript spz indicates the three dimensions: synergy combinations, postures and zones). If synergy i causes the arm to reach zone Z_k from posture j, $M^T_{\text{spz}}(i, j, k) = 1$, else it is 0.

The $N^T \times 49$ *Length Matrix*, L^T, stores the lengths of the generated trajectories, with $L^T(i, j)$ denoting the length of the trajectory generated from posture j by synergy i.

The $N^T \times 49$ *Curvature Matrix*, C^T, stores the curvatures of the generated trajectories, with $C^T(i, j)$ denoting the curvature of the trajectory generated from posture j by synergy i. The curvature is measured as the sum of the error estimates at set of points between the trajectory and its straight line fit.

Stage II: *Initial elimination*:

It is considered desirable that the basis synergies found should produce trajectories of relatively similar lengths and without significant curvature. To this end, synergies producing trajectories of widely varying lengths or very short or long lengths are removed, as are those producing trajectories with significant curvature. During deployment, the actual trajectory lengths can be varied by amplitude control, and curved trajectories obtained by a combination of synergies.

The mean length of the trajectories for synergy i is calculated as

$$\mu_i^L = \frac{1}{49}\sum_{j=1}^{49} L^T(i, j). \tag{35}$$

Similarly, the standard deviations of trajectory length are calculated as

$$\sigma_i^L = \sqrt{\frac{1}{49}\sum_{j=1}^{49}(L^T(i, j) - \mu_i^L)^2}. \tag{36}$$

Only those synergies whose mean length falls within a certain range $[\mu_1^L, \mu_2^L]$, and whose standard deviation is below a threshold level θ_σ^L are retained and the rest eliminated from the M^T_{spz} matrix, leaving a $N_L \times 49 \times 8$ *length-reduced zone performance matrix*, M^L_{spz} with N_L synergies, and the corresponding *Length-Reduced Curvature Matrix*, C^L.

The same procedure is then followed for curvature, using C^L to calculate the mean curvature:

$$\mu_i^C = \frac{1}{49}\sum_{j=1}^{49} C^L(i, j) \tag{37}$$

and curvature standard deviation

$$\sigma_i^C = \sqrt{\frac{1}{49}\sum_{j=1}^{49}(C^L(i, j) - \mu_i^C)^2} \tag{38}$$

for each synergy i. Only those synergies whose mean curvature is small and standard deviation below a threshold level θ_σ^C are retained and the rest eliminated from S_0, leaving a reduced synergy set, S_1 of N_R synergies with a $N_R \times 49 \times 8$ zone performance matrix $M_{\text{spz}}(S_1)$. The 8-bit binary vector χ_{ij} formed by the zone coverage bits in $M_{\text{spz}}(S_1)$ for synergy i and posture j is termed the *reach profile* for synergy i in posture j.

Please cite this article in press as: Byadarhaly, K. V., et al. A modular neural model of motor synergies. Neural Networks (2012), doi:10.1016/j.neunet.2012.02.003

Stage III: *Redundancy removal*:

As a first step towards meeting the requirement for minimum redundancy of basis synergies, a *synergy similarity matrix* (SSM), $E(S_1)$, is computed, with the ijth entry indicating the similarity between synergy i and synergy j in set S_1 as:

$$E_{ij}^{S} = 1 - \frac{1}{8 \times 49} \sum_{p=1}^{49} d_H(\chi_{ip},\ \chi_{jp}) \tag{39}$$

where $d_H(x,\ y)$ is the Hamming distance between vectors x and y and χ_{ip} and χ_{jp} the reach profiles for synergies i and j, respectively, from posture p. A value of $E_{ij} = 1$ for $i \neq j$ implies that the synergies involved have identical reach profiles across all postures. All subsets of synergies with mutually identical reach profiles are identified and only one synergy from each such set is retained. The rest are eliminated, giving a reduced synergy set S_2 with M synergies. Note that S_2 may still include synergies with very similar reach profiles, but we leave them in the set at this stage.

The $49 \times 8 \times M$ zone performance matrix $M_{\text{spz}}(S_2)$ is computed for the reduced synergy set, which provides reach profiles for all the synergies in it.

Stage IV: *Coverage evaluation*:

Next, the reduced synergy set, S_2, is evaluated for coverage across all postures. This information is used during subsequent steps.

The zone coverage provided by the synergy set S_2 is obtained by first logically summing the $M_{\text{spz}}(S_2)$ matrix along the synergies to give the 49×8 binary matrix, $Q_z(S_2)$:

$$Q_z(S_2) = \bigvee_{i=1}^{N_R} M_{\text{spz}}(i, j, k). \tag{40}$$

The 8-bit vector in row i of this matrix indicates which zones for posture i are reached by at least one synergy in S_2. It is termed the *base zone coverage profile* for posture i and is the logical sum of the reach profiles of all synergies in S_2 for posture i. The base zone coverage profile for each posture is checked to see if at least 3 well-separated zones are covered from it. If so, the posture is labeled *covered*, else *deficient*. This gives the 49-bit vector $q(S_2)$, where $q_j(S_2) = 1$ if posture j is covered by S_2 and 0 otherwise. This is termed the *base coverage profile vector*, and denoted by q^*. It should be noted that a posture that is deficient in S_2 will not be covered by the basis set either. Typically, this only happens for extremal corner postures.

A 49×1 *richness matrix*, $R(S_2)$ is also calculated by summing $Q(S_2)$ along all the zones, giving the number of zones reached by *all* the included synergies from each posture.

Stage V: *Iterative reduction*:

The goal in this stage is select a small set of basis synergies from S_2 such that the principles of maximum coverage and minimum redundancy are satisfied. This is done through an iterative split-and-select algorithm as follows:

1. Set the *current synergy set*, S, to S_2.

2. While the current synergy set is larger than N_{target}, do:

2.1. Randomly divide S into two subsets, S_A and S_B, of equal size.

2.2. Evaluate the coverage profile vectors (CPVs), $q(S_A)$ and $q(S_B)$, for the two subsets.

2.3. If neither subset has the same CPV as q^*, reset to Step 2.1.

Else, if one subset has the same CPV as q^*, set S to that subset.

Else, set S to the subset which has higher quality based on: (1) Higher total number of zones reached over all postures; and (2) Lower average similarity between synergies.

When the procedure ends, the set S is od size N_{target} and has the same coverage as S_2.

Stage VI: *Synergy augmentation*:

As noted earlier, the reduced synergy set S_2 used as the basis for the iterative reduction elimination process may have been deficient for some postures, and these deficiencies are mirrored in the final synergy set S. Therefore, if possible, S is augmented with a small number of synergies that had been eliminated in Stage I but remove the deficiencies in S.

The set S at this point is the desired set of basis synergies.

References

Albus, J. S. (1971). A theory of cerebellar function. *Mathematical Biosciences*, *10*, 25–61.
Asada, H., & Slotine, J. E. (1986). *Robot analysis and control*. New York, NY: Wiley Interscience.
Barto, A. G. (1995). Adaptive critics and the basal ganglia. In J. C. Houk, J. L. Davis, & D. G. Beiser (Eds.), *Models of information processing in the basal ganglia* (pp. 215–232). Cambridge, MA: MIT Press.
Bernstein, N. I. (1967). *The coordination and regulation of movements*. Oxford: Pergamon.
Bizzi, E., Cheung, V. C. K., d'Avella, H., Salitel, P., & Tresch, M. C. (2007). Combining modules for movement. *Brain Research Reviews*, *57*, 125–133.
Bullock, D., & Grossberg, S. (1988). Neural dynamics of planned arm movements: emergent invariants and speed-accuracy properties during trajectory formation. *Psychological Review*, *95*, 49–90.
Byadarhaly, K.V., Perdoor, M., & Minai, A.A. (2011). A neural model of motor synergies. In *Proceedings of IJCNN 2011* (pp. 2961–2968).
Byadarhaly, K.V., Perdoor, M., Vasa, S., Fernandez, E., & Minai, A.A. (2009). Learning complex population-coded sequences. In *Proceedings of the international conference on artificial neural networks* (pp. 296–305).
d'Avella, A., & Bizzi, E. (2005). Shared and specific muscle synergies in natural motor behaviors. *Proceedings of the National Academy of Sciences of the United States America*, *102*, 3076–3081.
d'Avella, A., Saltiel, P., & Bizzi, E. (2003). Combinations of muscle synergies in the construction of natural motor behavior. *Nature Neuroscience*, *6*, 300–308.
Doya, K., Katagiri, K., Wolpert, D.M., & Kawato, M. (2000a). Recognition and imitation of movement paterns by a multiple predictor-controller architecture. Tech. Rep. Instituteof Electronic Information and Communication Engineers TL2000-11, pp. 33–40.
Doya, K., Kimura, H., & Miyamura, A. (2001). Motor control: neural models and systems theory. *International Journal of Applied Mathematics and Computer Science*, *11*, 77–104.
Doya, K., Samejima, K., Katagiri, K., & Kawato, M. (2000b). Multiple model-based reinforcement learning. Tech. Rep. KDB-08. Kawato Dynamic Brain Project. ERATO. Japan Science and Technology Corporation.
Feldman, A. G., & Orlovsky, G. N. (1975). Activity of interneurons mediating reciprocal ia inhibition of motoneurons during locomotion. *Brain Research*, *84*, 181–194.
Flash, T., & Hogan, N. (1985). The coordination of arm movements: an experimentally confirmed mathematical model. *The Journal of Neuroscience*, *5*, 1688–1703.
Giszter, S. F., Moxon, K. A., Rybak, I. A., & Chapin, J. K. (2001). Neurobiological and neurorobotic approaches to control architectures for a humanoid motor system. *Robotics and Autonomous Systems*, *37*, 219–235.
Graybiel, A. M. (1995). Building action repertoires: memory and learning functions of the basal ganglia. *Current Opinion in Neurobiology*, *5*, 733–741.
Graziano, M. S. A. (2009). *The intelligent movement machine: an ethological perspective on the primate motor system*. Oxford, UK: Oxford University Press.
Grossberg, S., & Paine, R. W. (2000). A neural model of cortico-cerebellar interactions during attentive imitation and predictive learning of sequential handwriting movements. *Neural Networks*, *13*, 999–1046.
Haken, H., Kelso, J. A. S., & Bunz, H. (1985). A theoretical model of phase transitions in human hand movements. *Biological Cybernetics*, *51*, 347–356.
Hikosaka, O., Nakahara, H., Rand, M. K., Sakai, K., Lu, X., Nakamura, K., et al. (1999). Parallel neural networks for learning sequential procedures. *Trends in Neurosciences*, *22*, 464–471.
Houk, J. C. (2005). Agents of the mind. *Biological Cybernetics*, *92*, 427–437.
Houk, J. C., Adams, J. L., & Barto, A. G. (1995). A model of how the basal ganglia generate and use neural signals that predict reinforcement. In J. C. Houk, J. L. Davis, & D. G. Beiser (Eds.), *Models of information processing in the Basal Ganglia.* (pp. 249–270). Cambridge, MA: MIT Press.
Houk, J. C., & Wise, S. P. (1995). Distributed modular architectures linking basal ganglia, cerebellum and cerebral cortex: their role in planning and controlling action. *Cerebral Cortex*, *5*, 95–110.
Ijspeert, A., Nakanishi, J., & Schaal, S. (2003). learning attractor landscapes for learning motor primitives. In *Advances in neural information processing systems 15* (pp. 1547–1554). MIT Press.
Imamizu, H., Kuroda, T., Yoshioka, T., & Kawato, M. (2004). Functional magnetic resonance imaging examination of two modular architectures for switching multiple internal models. *The Journal of Neuroscience*, *24*, 1173–1181.
Ito, M. (1993). Movement and thought: identical control mechanisms by the cerebellum. *Trends in Neurosciences*, *16*, 448–450.

Please cite this article in press as: Byadarhaly, K. V., et al. A modular neural model of motor synergies. Neural Networks (2012), doi:10.1016/j.neunet.2012.02.003

Jordan, M. I., Flash, T., & Arnon, Y. (1994). A model of the learning of arm trajectories from spatial targets. *The Journal of Cognitive Neuroscience*, *6*, 359–376.
Karniel, A., & Inbar, G. F. (1997). A model for human reaching movements. *Biological Cybernetics*, *77*, 173–183.
Kawato, M., Furukawa, K., & Suzuki, R. (1987). A hierarchical neural network model for control and learning of voluntary movement. *Biological Cybernetics*, *68*, 95–103.
Kelso, J. A. S. (1995). *Dynamic patterns: the self-organization of brain and behavior*. Cambridge, MA: MIT Press.
Kelso, J. A. S. (2009). Synergies: atoms of brain and behavior. In D. Sternan (Ed.), *Progress in motor control: a multidisciplinary perspective* (pp. 83–91). Springer Verlag.
Krylow, M. A., & Zey Zymer, W. (1997). Role of intrinsic muscle properties in producing smooth movements. *IEEE Transactions on Biomedical Engineering*, *44*.
Li, W., & Todorov, E. (2004). Iterative linear quadratic regulator design for nonlinear biological movement systems. In *Proc. of the 1st international conference on informatics in control, automation and robotics, Vol.1* (pp. 222–229).
Li, W., Todorov, E., & Pan, X. (2004). Hierarchical optimal control of redundant biomechanical systems. In *Proc. of the 26th IEEE conference on engineering in medicine and biology society* (pp. 4618–4621).
Marr, D. (1969). A theory of cerebellar cortex. *Journal of Physiology*, *202*, 437–470.
Massone, L. L. E., & Myers, J. D. (1996). The role of plant properties in arm trajectory formation: a neural network study. *IEEE Transactions on Systems, Man and Cybernetics*, *26*, 719–732.
Meier, F., Theodorou, E., Stulp, F., & Schaal, S. (2011) Movement segmentation using a primitive library. In *IEEE/RSJ international conference on intelligent robots and systems, 2011*.
Minai, A.A., Perdoor, M., Byadarhaly, K.V., Vasa, S., & Iyer, L.R. (2010). A synergistic view of autonomous cognitive systems. In *Proceedings of IJCNN 2010* (pp. 498–505).
Morasso, P. (1992). Neural mechanisms of synergy formation. *Human Movement Science*, *11*, 169–180.
Muceli, S., Boye, A. T., d'Avella, A., & Farina, D. (2010). Identifying representative synergy matrices for describing muscular activation patterns during multi-directional reaching in the horizontal plane. *Journal of Neurophysiology*, *103*, 1532–1542.
Mussa-Ivaldi, F. (1999). A. modular features of motor control and learning. *Current Opinion in Neurobiology*, *9*, 713–717.
Orlovsky, G. N., Deliagina, T. G., & Grillner, S. (1999). *Neuronal control of locomotion: from mollusc to man*. Oxford, UK: Oxford University Press.
Pfeifer, R., & Bongard, J. (2006). *How the body shapes the way we think*. MIT Press.
Pratt, C. A., & Jordan, L. M. (1980). Recurrent inhibition of motor neurons in decerebrate cats during controlled treadmill locomotion. *Journal of Neurophysiology*, *44*, 489–500.
Schaal, S. (2003a). Dynamic movement primitives—a framework for motor control in humans and humanoid robots. In *International symposium on adaptive motion of animals and machines*.
Schaal, S. (2003b). Movement planning and imitation by shaping nonlinear attractors. In *Proceedings of the 12th Yale workshop on adaptive systems and learning*.
Schaal, S., Peters, J., Nakanishi, J., & Ijspeert, A. (2004). Learning movement primitives. In *International symposium on robotics research*, ISRR 2003. Springer.
Schlutz, A., Faulkner, J., & Kadhireshan, V.A. (1991). A simple hill element-nonlinear spring model of muscle contraction bio-mechanics. American Physiological Society 0161.
Schmidt, R. A., & Lee, T. D. (2005). *Motor control and learning: a behavioral emphasis*. Human Kinetics Publishers.
Schultz, W. (2000). Multiple reward signals in the brain. *Nature Reviews Neuroscience*, *1*, 199–207.
Schultz, W., Dayan, P., & Montague, P. R. (1997). A neural substrate of prediction and reward. *Science*, *275*, 1593–1599.
Schweighofer, N., Arbib, M. A., & Kawato, M. (1998a). Role of the cerebellum in reaching movements in humans i: distributed inverse dynamics control. *European Journal of Neuroscience*, *10*, 86–94.
Schweighofer, N., Spoelstra, J., Arbib, M. A., & Kawato, M. (1998b). Role of the cerebellum in reaching movements in humans ii: a neural model of the intermediate cerebellum. *European Journal of Neuroscience*, *10*, 95–105.
Shima, K., & Tanji, J. (2000). Neuronal activity in the supplementary and presupplementary motor areas for temporal organization of multiple movements. *Journal of Neurophysiology*, *84*, 2148–2160.
Sutton, R. S., & Barto, A. G. (1998). *Reinforcement learning*. Cambridge, MA: MIT Press.
Ting, L. H., & Macpherson, J. M. (2005). A limited set of muscle synergies for force control during a postural task. *Journal of Neurophysiology*, *93*, 609–613.
Todorov, E., & Jordan, M. I. (2002). Optimal feedback control as a theory of motor coordination. *Nature Neuroscience*, *5*, 1226–1235.
Torres-Oviedo, G., Macpherson, J. M., & Ting, L. H. (2006). Muscle synergy organization is robust across a variety of postural perturbations. *Journal of Neurophysiology*, *96*, 1530–1546.
Torres-Oviedo, G., & Ting, L. H. (2007). Muscle synergies characterizing human postural responses. *Journal of Neurophysiology*, *98*, 2144–2156.
Tresch, M. C., Cheung, V. C. K., & d'Avella, A. (2006). Matrix factorization algorithms for the identification of muscle synergies: evaluation on simulated and experimental data sets. *Journal of Neurophysiology*, *95*, 2199–2212.
Tresch, M. C., Salitel, P., & Bizzi, E. (1999). The construction of movement by the spinal cord. *Nature Neuroscience*, *2*, 162–167.
Tresch, M. C., Salitel, P., d'Avella, H., & Bizzi, E. (2002). Coordination and localization in spinal motor systems. *Brain Research Brain Research Reviews*, *40*, 66–79.
Turvey, M. T. (1990). Coordination. *American Psychologist*, *45*, 938–953.
Turvey, M. T., & Fonseca, S. (2009). The nature of motor control: perspectives and issues. *Advances in Experimental Medicine and Biology*, *629*, 92–123.
Vasa, S., Ma, T., Byadarhaly, K.V., Perdoor, M., & Minai, A.A. (2010). A spiking neural model for the spatial coding of cognitive response sequences. In *Proceedings of the IEEE international conference on development and learning* (pp. 140–146).
Winters, J. M., & Stark, L. (1987). Muscle models:what is gained and what is lost by varying muscle complexity. *Biological Cybernetics*, *55*, 403–420.
Wolpert, M. D., & Ghahramani, Z. (1997). Modular decomposition in visuomotor learning. *Nature*, *386*, 392–395.
Wolpert, M. D., Ghahramani, Z., & Flanagan, R. J. (2001). Perspectives and problems in motor learning. *Trends in Cognitive Sciences*, *5*, 487–494.
Wolpert, M. D., & Kawato, M. (1998). Multiple paired forward and inverse models for motor control. *Neural Networks*, *11*, 1317–1329.
Yuste, R., Maclean, J. N., Smith, J., & Lanser, A. (2005). The cortex as a central pattern generator. *Nature Reviews Neuroscience*, *6*, 477–483.

Please cite this article in press as: Byadarhaly, K. V., et al. A modular neural model of motor synergies. Neural Networks (2012), doi:10.1016/j.neunet.2012.02.003